Green Luminescence Band in ZnO: Fine Structures, Electron−Phonon Coupling, and Temperature Effect

S. L. Shi,[†] G. Q. Li,[†,‡] S. J. Xu,[*,†] Y. Zhao,[§] and G. H. Chen[§]

Department of Physics and HKU-CAS Joint Laboratory on New Materials, The University of Hong Kong, Pokfulam Road, Hong Kong, China, and Department of Chemistry and HKU-CAS Joint Laboratory on New Materials, The University of Hong Kong, Pokfulam Road, Hong Kong, China

Received: February 21, 2006; In Final Form: April 5, 2006

The green emission band of ZnO has been investigated by both experimental and theoretical means. Two sets of equally separated fine structures with the same periodicity (close to the longitudinal optical (LO) phonon energy of ZnO) are well resolved in the low-temperature broad green emission spectra. As the temperature increases, the fine structures gradually fade out and the whole green emission band becomes smooth at room temperature. An attempt to quantitatively reproduce the variable-temperature green emission spectra using the underdamped multimode Brownian oscillator model taking into account the quantum dissipation effect of the phonon bath is done. Results show that the two electronic transitions strongly coupled to lattice vibrations of ZnO lead to the observed broad emission band with fine structures. Excellent agreement between theory and experiment for the entire temperature range enables us to determine the dimensionless Huang−Rhys factor characterizing the strength of electron−LO phonon coupling and the coupling coefficient of the LO and bath modes.

Historically, zinc oxide (ZnO) is a technologically important material thanks to its piezoelectric characteristics and other unique properties such as its transparency up to the near ultraviolet (UV). It is also known that ZnO is a semiconductor with a wide band gap (∼3.37 eV) and an extremely large exciton binding energy (as high as 60 meV).[1] Recently, it has attracted renewed research interest due to its newly-found application potential in exciton-type short-wavelength optoelectronic devices that are functional at room temperature or above.[1−3] Despite a long history of industrial applications, a clear understanding of some fundamental properties of ZnO still remains elusive.[1,2,4−7] For example, contention still surrounds the microstructural origin.[4,8] To date, very different defect origins, such as the substitutional Cu^{2+} on the zinc site,[9] oxygen vacancy (V_O),[10] zinc vacancy (V_{Zn}),[11] and interstitial zinc (Zn_i),[12] have been suggested to be responsible for the green band of ZnO. Among them, the substitutional Cu^{2+} model proposed first by Dingle[9] has received much attention due to the distinct spectral features of a sharp zero-phonon line (ZPL) and a broad longitudinal optical (LO) phonon sideband at low temperature.[13−15] Taking into account only the coupling between one LO phonon mode and one electronic transition, Kuhnert and Helbig[13] employed a Poission distribution, $I_n = S^n e^{-S}/n!$, to fit the line shape of the green emission band and then obtained a Huang−Rhys factor of $S = 6.5$. It is well-known that the Poission distribution simply gives only a backbone of the absorption or luminescence line shape of the electron−LO phonon coupling system. Broadening due to acoustic-phonon-bath dissipation and the temperature effect cannot be accounted for in the model. Moreover, in addition to the first set of structures, the second set of structures with the same periodicity was also observed but its origin is not yet understood.[9,13] Full exploitation of ZnO in optoelectronic device applications certainly requires better knowledge of various optical processes in ZnO. Motivated by such a requirement, the present work is devoted to an enhanced understanding of the broad green luminescence band of ZnO. Employing a high-quality ZnO bulk crystal as the experimental sample, we measured its green emission band at various temperatures. Being very similar to the results in the literature,[9,13] two sets of equally separated fine structures are found to superimpose the broad green band. The energy separation between any two adjacent fine lines in each set is approximately the characteristic energy of the LO phonon in ZnO. To model the observed emission spectra at different temperatures, we adopted the multimode Brownian oscillator (MBO) model[16,17] taking into account both the electron−LO phonon coupling and the dissipative effect of the phonon-bath modes. Excellent agreement between theory and experiment is achieved when only two adjustable parameters were taken, namely, the dimensionless Huang−Rhys factor characterizing the electron−LO phonon coupling strength and the damping coefficient accounting for the bath dissipation.

The sample studied here is a high-quality ZnO bulk rod. Its band-edge emission from bound excitons is very intense and extremely narrow at low temperatures. Variable-temperature photoluminescence (PL) measurements of the sample have been performed in a high-resolution PL setup described elsewhere previously.[18] The excitation source is a 325 nm He−Cd laser. A standard lock-in amplification technique is employed in the PL measurements. Room-temperature Raman scattering measurements of the sample have been carried out under a backscattering geometry using a set of confocal micro-Raman systems, a detailed description of which can be found in our previous publication.[19]

Figure 1 shows the measured green emission band of the sample at various temperatures. To show the fine structures

* Corresponding author. E-mail: sjxu@hkucc.hku.hk.
[†] Department of Physics and HKU-CAS Joint Laboratory on New Materials.
[‡] Presently at Technische Universitat Chemnitz, Germany.
[§] Department of Chemistry and HKU-CAS Joint Laboratory on New Materials.

10.1021/jp0610968 CCC: $33.50
Published on Web 05/10/2006

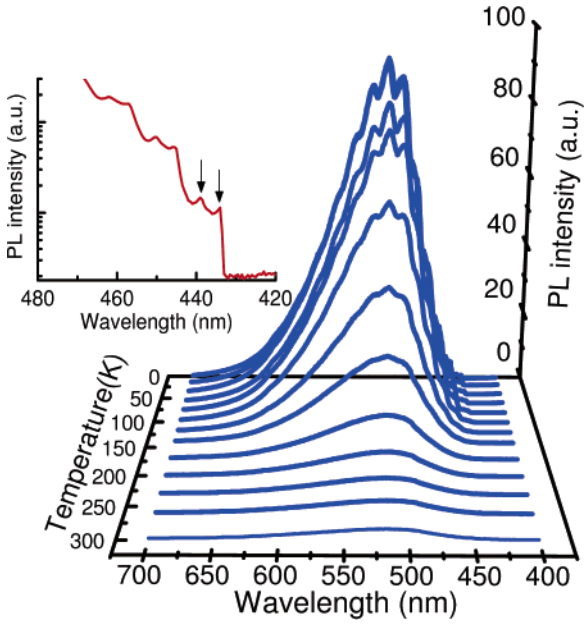

Figure 1. Measured green emission band at different temperatures. The inset shows an enlarged portion of the 5 K spectrum at the high-energy side. Two series of fine structures with a fixed energy separation of ~30 meV can be clearly resolved despite the fact that they superimpose the broad band.

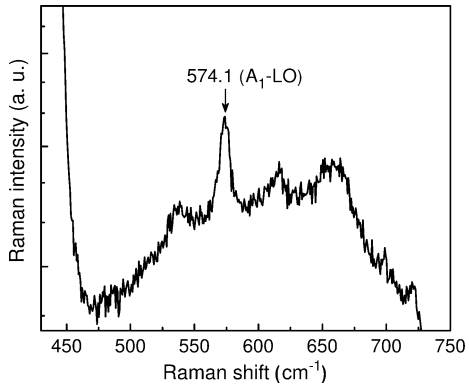

Figure 2. Measured Raman scattering spectrum of ZnO at room temperature. The A1-LO peak at 574.1 cm^{-1} is clearly seen.

clearly, an enlarged portion of the spectrum at the high-energy side is plotted in the inset. Indeed, the two well-resolved series of equally separated fine structures superimposing the broad band can be observed at the high-energy side. The energy spacing between the two series is ~30 meV, while the energy separation between any two adjacent lines in the fine structure of either series is found to be ~71 meV. The latter approximately equals the characteristic energy (574.1 cm^{-1} or 71.2 meV) of the A1-LO mode which is revealed by the Raman scattering spectrum of ZnO in Figure 2. This energy value of the A1-LO mode is also consistent with the value reported in the literature.[20] Obviously, the appearance of the LO phonon structure indicates that the broad green emission band is associated with strong electron−LO phonon coupling. Furthermore, observation of the two sets of fine structures with an energy separation of 30 meV postulates that two electronic transitions coupled with the lattice vibration exist. Examining the temperature dependence of the green emission band is of great importance to understanding its physical origin.

As shown in Figure 1, the green emission band exhibits several spectral variations as the lattice temperature increases. First, its total integrated intensity decreases gradually with increasing temperature. This is the usual temperature behavior of semiconductor luminescence due to several quenching mechanisms such as thermal activation of some nonradiative centers and thermal escaping of localized carriers involved in the emission process.[21] Second, the fine structures fade out gradually and become no longer observable when the temperature is above 140 K. As will be proved later, it is due to thermal broadening of each vibronic transition. Third, the peak position of the emission band remains unchanged when the temperature is not higher than 200 K. For high temperatures, the peak position tends to blue shift with increasing temperature. It can be explained as being a result of populating the higher vibronic states.[21] For the purpose of calculating the green emission band in ZnO, the luminescent system can be simplified by a physical model in which composite quasi-particles formed by strong electron−LO phonon coupling are dissipated by a phonon bath. For such a model system, its optical response function can be calculated using a MBO model with Markovian dissipation.[16,17,22]

On the basis of the classic work of Lax[23] and Kubo,[24] the MBO model introduces dissipation mechanisms that are omnipresent in real solids into a harmonic oscillator system by coupling the system oscillators linearly to bath modes with a continuous spectrum. In such a model system, there is a two-electronic-level system with some primary nuclear coordinates coupled linearly to it and to the harmonic bath. The Hamiltonian of the system is given by[16,17]

$$H = |g\rangle H_g \langle g| + |e\rangle H_e \langle e| + H' \tag{1}$$

where

$$H_g = \sum_j \left[\frac{p_j^2}{2m_j} + \frac{1}{2} m_j \omega_j^2 q_j^2 \right] \tag{2}$$

$$H_e = \hbar\omega_{eg}^0 + \sum_j \left[\frac{p_j^2}{2m_j} + \frac{1}{2} m_j \omega_j^2 (q_j + d_j)^2 \right] \tag{3}$$

and

$$H' = \sum_n \left[\frac{P_n^2}{2m_n} + \frac{1}{2} m_n \omega_n^2 \left(Q_n - \sum_j \frac{c_{nj} q_j}{m_n \omega_n^2} \right)^2 \right] \tag{4}$$

Here, p_j (P_n), q_j (Q_n), m_j (m_n), and ω_j (ω_n) are the momentum, the coordinate, the mass, and the angular frequency of the jth (nth) nuclear mode of the primary (bath) oscillators, respectively. d_j represents the displacement for the jth nuclear mode in the excited electronic state. $\hbar\omega_{eg}^0$ is the energy separation of the purely electronic levels. H' describes the bath modes and their coupling to the primary oscillators with a coupling strength of c_{nj}. The cross-terms in $q_j Q_n$ are responsible for damping.[25] An energy gap coordinate operator, U, is defined as

$$U = H_e - H_g - \hbar\omega_{eg}^0 \tag{5}$$

The linear absorption spectrum and the relaxed photoluminescence spectrum can be computed by truncating the cumulant expansion of the spectral response function at second order (see ref 16, Appendix 8B). Before deriving the expression of the absorption or photoluminescence line shape, we first define a

correlation function:

$$C_j(t) = -\frac{1}{2\hbar^2}[\langle U(t)\, U(0)\rho_g\rangle - \langle U(0)\, U(t)\rho_g\rangle] \quad (6)$$

where $U(t)$ is the operator U in the interaction representation and ρ_g is the equilibrium ground-state vibrational density matrix:

$$\rho_g = \frac{|g\rangle\langle g|\exp(-\beta\hat{H}_g)}{\mathrm{Tr}[\exp(-\beta\hat{H}_g)]} \quad (7)$$

with $\beta = 1/k_BT$. The Fourier transform of the correlation function, $C_j(t)$, has an imaginary part known as the spectral density:

$$\tilde{C}_j''(\omega) = \frac{2\lambda_j\omega_j^2\omega\gamma_j(\omega)}{\omega^2\gamma_j^2(\omega) + [\omega_j^2 + \omega\Gamma_j(\omega) - \omega^2]^2} \quad (8)$$

Here, $2\lambda_j$ is the jth mode contribution to the Stokes shift

$$2\lambda_j = \frac{m_j\omega_j^2 d_j^2}{\hbar} \quad (9)$$

$\Gamma_j(\omega)$ is the real part of the self-energy. One can alternatively write $\lambda_j = S_j\hbar\omega_j$, where S_j is the well-known dimensionless Huang−Rhys factor characterizing the strength of electron−LO phonon interactions.[26,27] $\gamma_j(\omega)$ is the spectral distribution function describing the coupling between the primary oscillator and the secondary bath oscillators. In the present study, we adopt a simple form of the MBO model in which only a single primary oscillator (i.e., LO phonon) is considered and its coupling strength with the bath modes is assumed to be a constant (i.e., $\gamma_j(\omega) =$ constant, called Markovian or Ohmic limit) to compute PL spectra. For this simple case, the spectral density function reads[17]

$$C''(\omega) = \frac{2\lambda_l\omega_l^2\omega\gamma_l}{\omega^2\gamma_l^2 + (\omega_l^2 - \omega^2)^2} \quad (10)$$

where the real part of the self-energy, $\Gamma_j(\omega)$, is set to zero.

The spectral response function, $g(t)$, can be expressed in terms of the frequency-domain correlation function, $C''(\omega)$,

$$g(t) = -\frac{1}{2\pi}\int_{-\infty}^{\infty} d\omega\, \frac{C''(\omega)}{\omega^2}[1 + \coth(\beta\hbar\omega/2)][e^{-i\omega t} + i\omega t - 1] \quad (11)$$

The PL line shape can be then obtained from the spectral response function, $g(t)$:

$$I_{PL}(\omega) = \frac{1}{\pi}\mathrm{Re}\int_0^{\infty} \exp[i(\omega - \omega_{eg}^0 + \lambda)t - g^*(t)]\, dt \quad (12)$$

Using eq 12, we calculated the green emission band of ZnO at different temperatures. The parameters used in the calculations are $S_1 = 6.4$, $\gamma_1 = 65$ cm^{-1}, $\hbar\omega_{e1g}^0 = 2.825$ eV, $S_2 = 6.4$, $\gamma_2 = 60$ cm^{-1}, and $\hbar\omega_{e2g}^0 = 2.855$ eV for temperatures below 200 K. It should be noted that the Huang−Rhys factor for lower temperatures determined in the present study is almost identical to the value $S = 6.5$ obtained by Kuhnert and Helbig using a simple Poission distribution fit.[13] The energetic positions of the two ZPL lines are also consistent with those in the literature.[9,13] For temperatures above 200 K, both S_1 and S_2 were adjusted to 7 while $\hbar\omega_{e1g}^0$ and $\hbar\omega_{e2g}^0$ were changed to 2.841 and 2.871 eV, respectively. For the entire temperature range, $\hbar\omega_{LO}$ (~574 cm^{-1}), γ_1 and γ_2 remain unchanged for the two electronic transitions (i.e., $\hbar\omega_{e1g}^0$ and $\hbar\omega_{e2g}^0$). The weight coefficients used in the calculations of overall emission spectra are 1 and 1.5 for $\hbar\omega_{e1g}^0$ and $\hbar\omega_{e2g}^0$, respectively. The calculated spectra (solid lines) are plotted in Figure 3 where the measured spectra (open circles) are also given for a direct comparison. It can be seen that excellent agreement between theory and experiment is achieved, which indicates that the linear coupling approximation of electron−LO phonon interactions and the Markovian assumption of the dissipative bath give a satisfactory explanation of the green emission band of ZnO. From the large values of the Huang−Rhys factor obtained from the calculations, we understand that very strong electron−LO phonon coupling is responsible for the observed broad green emission band in ZnO. Furthermore, the transition energies of purely electronic transitions (often called zero-phonon lines in the literature) are far below the fundamental band gap (~3.37 eV) of ZnO, implying that electrons responsible for the green emission band are localized around certain deep centers such as the substitutional Cu^{2+} on the zinc site proposed by Dingle.[9] Determination of the Huang−Rhys factor for the green emission band of ZnO by rigorous theoretical means from the experimental spectra also enables us to conclude that large lattice relaxation takes place accompanying the radiative decaying of localized electrons in ZnO.

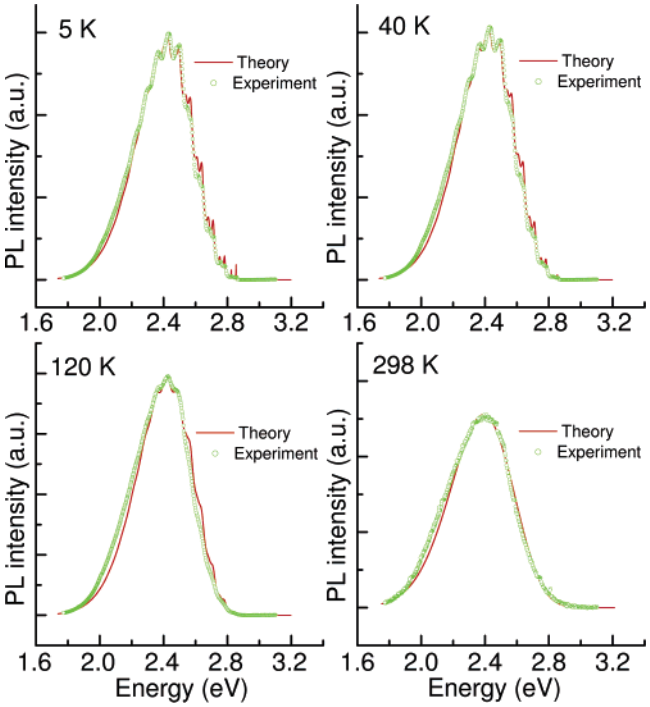

Figure 3. Measured and calculated emission spectra of the samples for several temperatures. The open circles represent the measured spectra, while the solid lines are the calculated spectra using the MBO model.

In conclusion, the green emission band of ZnO bulk crystal has been investigated in detail. Two sets of equally separated fine structures superimposing the broad band have been observed, and excellent agreement between theory and experiment has been obtained using the multimode Brownian oscillator model. It is suggested that the two electronic transitions strongly coupled to the lattice vibrations of ZnO are responsible for the broad green emission band.

Acknowledgment. The work was supported by HK RGC-CERG (Grant No. HKU 7036/03P). One of the authors, S.J.X.,

wishes to thank M. H. Xie for providing the ZnO sample used in this study.

Note Added after ASAP Publication. This Article was published on Articles ASAP on May 10, 2006. $\gamma_j(\omega)$ in the denominator of eq 8 and in the lines of text after eq 9 and after eq 10 was changed to $\Gamma_j(\omega)$. The corrected Article was reposted May 15, 2006.

References and Notes

(1) See, for example, a recent review article: Look, D. C. *Mater. Sci. Eng., B* **2001**, *80*, 383 and references therein.
(2) Norton, D. P.; Heo, Y. W.; Ivill, M. P.; Ip, K.; Pearton, S. J.; Chisholm, M. F.; Steiner, T. *Mater. Today* **2004**, *7*, 34.
(3) Wang, Z. L. *J. Phys.: Condens. Matter* **2004**, *16*, R829.
(4) Li, D.; Leung, Y. H.; Djurisic, A. B.; Liu, Z. T.; Xie, M. H.; Shi, S. L.; Xu, S. J.; Chan, W. K. *Appl. Phys. Lett.* **2004**, *85*, 1601.
(5) Xu, S. J.; Xiong, S.-J.; Shi, S. L. *J. Chem. Phys.* **2005**, *123*, 221105.
(6) Dai, D. C.; Xu, S. J.; Shi, S. L.; Xie, M. H.; Che, C. M. *Opt. Lett.* **2005**, *30*, 3377.
(7) Fan, W. J.; Xia, J. B.; Agus, P. A.; Tan, S. T.; Yu, S. F.; Sun, X. W. *J. Appl. Phys.* **2006**, *99*, 013702.
(8) Kohan, A. F.; Ceder, G.; Morgan, D.; Van de Walle, C. G. *Phys. Rev. B* **2000**, *61*, 15019.
(9) Dingle, R. *Phys. Rev. Lett.* **1969**, *23*, 579.
(10) Vanheusden, K.; Seager, C. H.; Warren, W. L.; Tallant, D. R.; Voiget, J. A. *Appl. Phys. Lett.* **1996**, *68*, 403.
(11) Bylander, E. G. *J. Appl. Phys.* **1978**, *49*, 1188.
(12) Liu, M.; Kitai, A. H.; Mascher, P. *J. Lumin.* **1992**, *54*, 35.
(13) Kuhnert, R.; Helbig, R. *J. Lumin.* **1981**, *26*, 203.
(14) Robbins, D. J.; Herbert, D. C.; Dean, P. J. *J. Phys. C: Solid State Phys.* **1981**, *14*, 2859.
(15) Klingshirn, C. *Semiconductor Optics*, 2nd ed.; Springer: Germany, 2005; p 356.
(16) Mukamel, S. *Principles of Nonlinear Optical Spectroscopy*; Oxford University Press: Oxford, U.K., 1995; p 226.
(17) Zhao, Y.; Knox, R. S. *J. Phys. Chem. A* **2000**, *104*, 7751.
(18) Xu, S. J.; Liu, W.; Li, M. F. *Appl. Phys. Lett.* **2000**, *77*, 3376.
(19) Zhao, D. G.; Xu, S. J.; Xie, M. H.; Tong, S. Y.; Yang, H. *Appl. Phys. Lett.* **2003**, *83*, 677.
(20) Calleja, J. M.; Cardona, M. *Phys. Rev. B* **1977**, *16*, 3753.
(21) Li, Q.; Xu, S. J.; Xie, M. H.; Tong, S. Y. *Europhys. Lett.* **2005**, *71*, 994.
(22) Toutounji, M. M.; Small, G. J. *J. Chem. Phys.* **2002**, *117*, 3848.
(23) Lax, M. *J. Chem. Phys.* **1952**, *20*, 1752.
(24) Kubo, R. *J. Phys. Soc. Jpn.* **1954**, *20*, 935.
(25) Knox, R. S.; Small, G. J.; Mukamel, S. *Chem. Phys.* **2002**, *281*, 1.
(26) Huang, K.; Rhys, A. *Proc. R. Soc. London, Ser. A* **1950**, *204*, 406.
(27) Zhao, Y.; Brown, D. W.; Lindenberg, K. *J. Chem. Phys.* **1997**, *107*, 3159; **1997**, *107*, 3179; **1997**, *106*, 5622.